Short-term pulse rate variability is better characterized by functional near-infrared spectroscopy than by photoplethysmography

Lisa Holper
Erich Seifritz
Felix Scholkmann

SPIE.

Short-term pulse rate variability is better characterized by functional near-infrared spectroscopy than by photoplethysmography

Lisa Holper,[a,][*] Erich Seifritz,[a] and Felix Scholkmann[b]
[a]University of Zurich, Department of Psychiatry, Psychotherapy, and Psychosomatics, Hospital of Psychiatry, Lenggstrasse 31, 8032 Zurich, Switzerland
[b]University Hospital Zurich, University of Zurich, Biomedical Optics Research Laboratory, Department of Neonatology, Frauenklinikstrasse 10, 8091 Zurich, Switzerland

Abstract. Pulse rate variability (PRV) can be extracted from functional near-infrared spectroscopy (fNIRS) (PRV_{NIRS}) and photoplethysmography (PPG) (PRV_{PPG}) signals. The present study compared the accuracy of simultaneously acquired PRV_{NIRS} and PRV_{PPG}, and evaluated their different characterizations of the sympathetic (SNS) and parasympathetic (PSNS) autonomous nervous system activity. Ten healthy subjects were recorded during resting-state (RS) and respiratory challenges in two temperature conditions, i.e., room temperature (23°C) and cold temperature (4°C). PRV_{NIRS} was recorded based on fNIRS measurement on the head, whereas PRV_{PPG} was determined based on PPG measured at the finger. Accuracy between PRV_{NIRS} and PRV_{PPG}, as assessed by cross-covariance and cross-sample entropy, demonstrated a high degree of correlation ($r > 0.9$), which was significantly reduced by respiration and cold temperature. Characterization of SNS and PSNS using frequency-domain, time-domain, and nonlinear methods showed that PRV_{NIRS} provided significantly better information on increasing PSNS activity in response to respiration and cold temperature than PRV_{PPG}. The findings show that PRV_{NIRS} may outperform PRV_{PPG} under conditions in which respiration and temperature changes are present, and may, therefore, be advantageous in research and clinical settings, especially if characterization of the autonomous nervous system is desired. © 2016 Society of Photo-Optical Instrumentation Engineers (SPIE) [DOI: 10.1117/1.JBO.21.9.091308]

Keywords: heart rate variability; functional near-infrared spectroscopy photoplethysmography; autonomous nervous system.

Paper 160042SSRR received Jan. 22, 2016; accepted for publication Apr. 18, 2016; published online May 17, 2016.

1 Introduction

Heart rate variability (HRV), i.e., the variations in the inter-beat-interval of the heart rate (HR), is a physiological phenomenon. The usefulness of HRV as a tool for basic research as well as for medical diagnostic purposes to assess the function of the autonomic nervous system has been verified in numerous studies.[1–4] The gold standard is the analysis of interbeat (RR) intervals derived from electrocardiography (ECG). Alternatively, pulse cycle intervals variability based on blood flow pulsations (i.e., PRV) can be derived from pulse oximetry, i.e., photoplethysmography (PPG) (PRV_{PPG}). PRV_{PPG} is convenient, noninvasive, and widely available and has, therefore, been suggested for simplifying ambulatory HRV monitoring.[5–7] Under resting conditions, recordings derived from PPG and ECG demonstrate a high degree of correlation ($\sim r > 0.93$).[7,8] However, PRV_{PPG} also has disadvantages. While sufficient accuracy can be obtained when subjects are under optimal resting conditions, PRV_{PPG} has been reported to be vulnerable to motion artifacts,[6] physical exercise,[5] or mental stressors,[7] making it considerably less accurate compared to ECG. The smaller accuracy may arise due to probe instability, sweating, artifacts during exercise, and the influence of different cardiovascular components. Furthermore, the accuracy has been reported to particularly decrease for high frequency (HF) or short-term variability; in other words, PRV_{PPG} has been shown to have a smaller accuracy

in particular for the contributions of the parasympathetic nervous system (PSNS)[7,9] compared to the HRV derived from ECG.

The sympathetic nervous system (SNS) and PSNS have profound impacts on HRV and thus PRV. For example, decreased SNS activity or increased PSNS activity typically results in a reduction versus an increase of HRV. To characterize the contributions of the SNS and PSNS on HRV and PRV, frequency-domain methods have been typically applied. Activity in the HF band (0.15 to 0.40 Hz) can be associated with increased PSNS activation. For example, variation of HF can be driven by respiratory changes that modulate HRV and PRV via increases or decreases in PSNS activity.[10–12] Similarly, exposure to cold temperature leads to a reduction in HRV and PRV via increased PSNS activity in order to save and restore body energy. The relationship between the HF component and the PSNS state is thereby mainly caused by the cardiac PSNS's input and thus not directly reflects the parasympathetic "tone" *per se*.[13] Activity in the low frequency (LF) band (0.04 to 0.15 Hz), in contrast, in thought to represent a mixture of the modulation of both SNS and PSNS.[14] Therefore, the ratio between LF and HF (LF/HF ratio) has been suggested to reflect an approximation of the association between SNS and PSNS.[15–17] However, recent studies reported that the LF/HF ratio does not accurately measure cardiac SNS-PSNS balance.[14,18,19] Based on this, the SDNN/RMSSD has been proposed as another surrogate measure for the LF/HF ratio in the time-domain.[20]

*Address all correspondence to: Lisa Holper, E-mail: lisa.holper@puk.zh.ch

Whereas SDNN (i.e., the standard deviation of normal to normal RR intervals) is thought to represent characteristics of long-term HRV and PRV changes, RMSSD (i.e., the root mean square of successive heartbeat interval differences) is associated with short-term HRV and PRV changes. The SDNN/RMSSD ratio is, therefore, thought to represent the balance between long-term and short-term variabilities and thus represents the SNS-PSNS balance.[21]

The two described measures can be related to one of the most commonly used method for analyzing HRV and PRV, i.e., Poincaré plots. Poincaré plots are graphical illustrations of two consecutive RR intervals and are valuable due to their ability of displaying the nonlinear aspects of HRV and PRV sequences.[22] The typical elongated shape of a Poincaré plot can be evaluated numerically using an ellipse fitting technique that provides a ratio of two standard deviations, i.e., the ratio between the dispersion (standard deviation) on the minor axis (SD1) and on the major axis (SD2), called the SD1/SD2 ratio. Whereas SD1 represents the short-term HRV and PRV thought to reflect PSNS activity, SD2 represents the long-term HRV and PRV thought to reflect SNS activity, with the SD1/SD2 ratio denoting the SNS-PSNS balance.

Finally, based on the SD1 and SD2 parameters, yet another measure has been recently proposed, the complex correlation measure (CCM).[23,24] CCM is a nonlinear HRV and PRV measure that quantifies the temporal aspects of Poincaré plots. In contrast to SD1 and SD2, CCM measures the beat-to-beat dynamics and is particularly thought to have a greater sensitivity to changes in PSNS activity.

In the present analysis, we aimed to apply the described linear and nonlinear measures to examine the accuracy and characterize the contributions of the SNS and PSNS of PRV_{PPG} in comparison to PRV derived from functional near-infrared spectroscopy (fNIRS) (PRV_{NIRS}).

So far, PRV quantitation using fNIRS has been investigated in two studies. Trajkovic et al.[25] quantified the correlation between PPG (and HRV, respectively) signals derived from simultaneously acquired fNIRS and ECG in 11 healthy adults and reported a high correlation ($r > 0.98$). Perdue et al.[26] investigated simultaneously acquired fNIRS-based pulse activity and ECG-based heart activity in 10 healthy infants and reported not only a high correlation during the RS (median $r = 0.90$), but also during visual stimulation (median $r = 0.981$), despite high levels of movements typically occurring in infants.

To characterize the contributions of the SNS and PSNS on the PRV, the present study assessed the impact of changes in respiration and temperature on the PRV, which are both important variables affecting PRV via the SNS and PSNS.[27] Changes in respiration were induced by respiratory challenges, i.e., hyperventilation (HV), breath-holding (BH), and rebreathing (RB) compared to RS. Changes in temperature were induced by changing the environmental (i.e., room) temperature (23°C versus 4°C). PRV_{NIRS} was measured on the head and PRV_{PPG} was measured on the finger.

By addressing both the accuracy and contributions of the autonomic nervous system, we hypothesized to provide meaningful information on the performance of PRV_{NIRS} and PRV_{PPG}. In particular, we hypothesized that both changes in respiration and temperature would elicit larger short-term variability (HF, RMSSD, and SD1) reflecting increased PSNS activity, and that PRV_{NIRS} may characterize these changes better compared

to PRV_{PPG}, due to the known drawbacks of motion artifacts in PRV_{PPG}. Extracting PRV_{NIRS} may further be advantageous for both research and clinical settings, as fNIRS is a brain imaging method at the same time, which would enable to measure both brain activity and PRV simultaneously.

2 Materials and Methods

2.1 Subjects

Ten healthy subjects (age 32 ± 2.3 years, five females) were recruited at the University of Zurich. Exclusion criteria were any psychiatric or neurological disorder or current medication. All subjects gave written informed consent. The study was approved by the ethics committee of the Canton Zurich (KEK-ZH-Nr: 2014-0056) and conducted in accordance with the Declaration of Helsinki.

2.2 Experimental Protocol

Each subject underwent two experimental series separated by 1 week. Both experimental conditions were conducted at the same day and time between 9:00 and 12:00 am with a total duration of 10 min. Subjects were seated in a comfortable chair with the head positioned in a head rest in order to minimize head motion; this postural position was maintained during the whole experiment.

- CONTROL temperature: The first experimental series was conducted at a room temperature of 23°C.
- COLD temperature: The second experimental series was conducted at a cold temperature of 4°C within a cold storage room.

In both temperature conditions, subjects wore regular street wear and there was no other difference in the setup between the conditions. The following four respiratory challenges were assessed in each condition:

- RS (5 min) consisted of subjects sitting still with eyes open with normal breathing (60 s break interval, ∼15 cycles/min).
- HV consisted of one period of rapidly breathing in and out with constant respiratory volume (30 s, ∼60 cycles/min) followed by normal breathing (60 s break interval).
- BH consisted of one period of breath hold (30 s, no breathing) followed by normal breathing (60 s break interval).
- RB consisted of one period of breathing in an RB bag (3 L) (30 s, respiration rate did not differ from normal breathing, i.e., ∼15 cycles/min) followed by normal breathing (60 s break interval).

For BH and RB, subjects were trained prior to recording to perform the inspirational volume of air before the challenge similar to a normal breath cycle, in order to avoid inhaling a larger volume of air than the volume of a normal breath cycle.

2.3 Functional Near-Infrared Spectroscopy Instrumentation

An NIRSport instrument (LLC NIRx Medical Technologies) was used for the fNIRS recordings. The system utilized
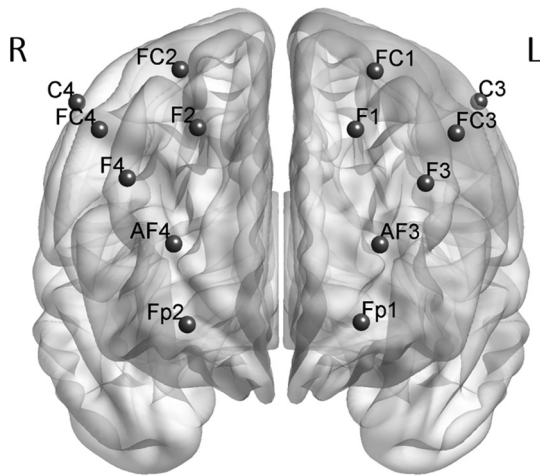
Fig. 1 fNIRS channel positions. Channel setup covering the prefrontal cortex (channels indicate the middle between source and detector). The MATLAB® toolbox NFRI[28] was used to estimate the MNI coordinates of the used EEG 10 to 20 position. Channel positions were visualized using BrainNet Viewer.[29]

time-multiplexed dual-wavelength light-emitting diodes. Each diode contained two light sources with wavelengths of 760 and 850 nm. Optical detection was performed with photoelectrical detectors containing silicon photodiodes (Siemens, Germany). Sources and detectors were placed in a head cap to allow for direct skin contact (Epitex Inc., Japan). The data acquisition board was connected to a notebook computer running LabVIEW 2011 (National Instruments, Austin, Texas). The fNIRS data were recorded with a sampling frequency of 7.81 Hz. The probe setup covered parts of the prefrontal cortex (Fig. 1). Functional recordings were visually inspected for motion artifacts (in particular, "steps" and "spikes") without the need for removal of artifacts. The time series of oxyhemoglobin (O_2Hb) were then used to extract HRV (Sec. 2.4).

2.4 Pulse Rate Variability Extraction from Functional Near-Infrared Spectroscopy

PRV_{NIRS} was extracted using the automatic multiscale-based peak detection (AMPD) algorithm developed by Scholkmann et al.[30] AMPD is based on the calculation and analysis of the local HR maxima in the raw fNIRS time series. AMPD detects the HR peaks, which are then used to calculate the interpeak

intervals frequency via interpolating the time difference signal. The first step of the AMPD algorithm consists of calculating the local maxima scalogram (LMS). To this end, the signal is first linearly detrended in that the least-squares fit of a straight line to a given raw O_2Hb signal is calculated and subtracted from the signal. The local maxima of the signal are then determined using a moving window approach. The second step of the algorithm comprises a row-wise summation of the LMS matrix resulting in a vector v. The global minimum λ of the vector v represents the scale with the most local maxima, which is then used in the third step to reshape the LMS matrix by removing all elements larger than λ. In the last step of the algorithm, the HR peaks are detected by calculating the columnwise standard deviation of the LMS matrix. Each point of the total number of detected peaks of a given signal indicated the values of the detected peaks (Fig. 2). The AMPD calculation was done for each of the channels (i.e., 1 to 16) and for each subject. Channels without cardiac components due to noise were identified and excluded from analysis. A final PRV_{NIRS} estimate was obtained for each single subject by computing the median PRV over all channels at each time point.

2.5 Photoplethysmography-Derived Pulse Rate Variability

A LifeSense LS1-9R multiparameter instrument (Nonin Medical, Sweden) was used to derive HR from finger PPG. Subjects wore a finger pulse oximeter through which HR were sampled at 10 Hz. Triggers were logged to allow for temporal synchronization with the fNIRS data. For statistical analysis, HR values were automatically computed by the LifeSense instrument from the raw data.

3 Data Analysis

Data collection and statistical analysis were performed in accordance with the Task Force Guidelines of The European Society of Cardiology and the North American Society of Pacing and Electrophysiology[31] and the related literature.[32,33]

Statistical analysis was performed using MATLAB® (Version 2015b, MathWorks). All methods were applied on the single-subject level, and presented on the group-level. The analysis included the RS series (5 min), HV, BH, and RB (each 30 s). The break intervals between the respiratory challenges were not included in the analysis. Statistical significance was assessed using repeated measures ANOVA with the
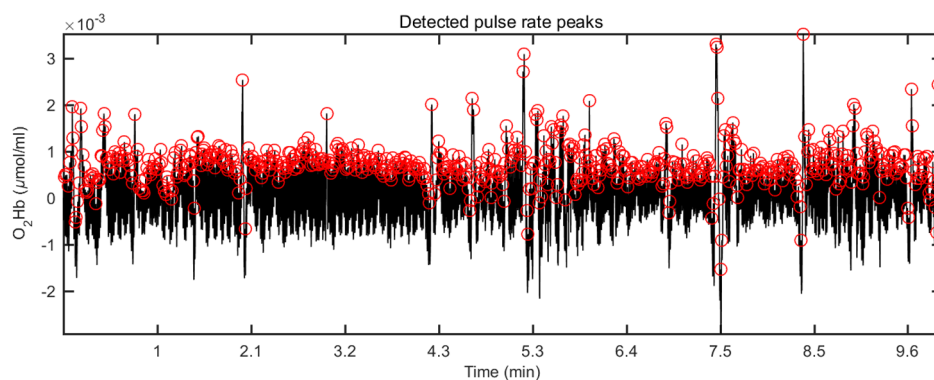
Fig. 2 PRV-extraction from fNIRS. Illustration of the results of applying the AMPD algorithm[30] to raw fNIRS time series to calculate PRV_{NIRS}. Red dots represent the detected HR peaks in a given signal with the peaks indicating the values of PRV at each point.

between-subject factor "temperature" (CONTROL versus COLD) and the within-subject factor "respiration" (RS, HV, BH, and RB). In the case of significance, a paired t-test was used as *post hoc* comparison. To illustrate the performance of PRV_{NIRS} and PRV_{PPG}, receiver operating characteristic (ROC) curves were generated based on logistic regression using the binary classifier "temperature" (CONTROL versus COLD). The significance level was considered to be $p < 0.05$.

3.1 Accuracy Between Pulse Rate Variability Measures

3.1.1 Cross-covariance

Normalized cross-covariance (C-COV) was quantified to assess the accuracy between PRV_{NIRS} and PRV_{PPG} as suggested by Perdue et al.[26] The covariance was scaled; hence, the auto-covariance was 1 for each signal at time lag 0. The time lag between the two traces was allowed to vary, and the highest correlation coefficient (r) was reported. Coefficients higher than $r > 0.3$ were considered moderate, coefficients higher than $r > 0.7$ were considered large. A mean time lag of 0.4 ± 4.6 s was found between PRV_{NIRS} and PRV_{PPG}. The smallest time lags were observed in the RS, but there were overall no significant lag-differences between the RS, the respiratory challenges, or the temperature change. Perdue et al.[26] suggested that this delay is due to the slow hemodynamic response time that may vary between subjects and may be dependent upon variations in subject blood vessels.

3.1.2 Cross-sample entropy

Cross-sample entropy (C-SampEn) was applied as a nonlinear measure to quantify the regularity or synchronicity in the potentially nonstationary PRV signals.[34] Entropy-based measures have been widely used for the analysis of physiological time series to explore the complexity between two time-series.[35,36] C-SampEn measures the relative regularity of two signals, with lower C-SampEn values denoting greater conditional regularity or synchronicity, whereas higher values implicate that the given signals are less predictable (or more complex). While C-SampEn may be intuitively understood as the opposite of temporal correlation, it does not assume that signals are temporally stationary processes, but provides an alternative and complementary measure to assess the nonlinear statistics of PRV.[37–39]

3.2 Sympathetic and Parasympathetic Autonomous Nervous System Contributions on Pulse Rate Variability

The following measures of short-term and long-term variabilities were assessed only in the RS series. The respiratory challenges were analyzed only with respect to the short-term variability (see rationale in Secs. 3.2.1 and 3.2.2).

3.2.1 Frequency-domain (low frequency/high frequency ratio)

Power spectral density (PSD) in the frequency-domain was applied to calculate the averaged power in the HF band (0.15 to 0.4 Hz) and the LF band (0.04 to 0.15 Hz). We applied the Lomb-Scargle power spectral density (LS-PSD) estimate that has been proposed as a more appropriate method for HRV compared to classical fast Fourier transform-based methods,[40] since it can be used without the need to resample and to detrend the typically unevenly sampled HRV time series.

PSD only provides an accurate estimation when the signal is supposed to maintain stationarity, which typically requires long-term recordings. Recordings should be at least 10 times the wavelength of the lowest frequency bound of interest. Thus, recordings of ~1 min are needed to assess the HF components (i.e., a lowest bound of 0.15 Hz is a cycle of 6.6 s, therefore 10 cycles require ~60 s), while more than 4 min are needed to address the LF component (with a lower bound of 0.04 Hz). In the present analysis, we, therefore, only analyzed the RS series (5 min, consisting of at least 256 samples[32]).

3.2.2 Time-domain (SDNN/RMSSD ratio)

As suggested by Wang and Huang,[20] the two surrogate indices, SDNN and RMSSD, in the time-domain were computed. Analysis was performed using the HRVAS toolbox.[41] Analog to the frequency-domain, very short time series may not provide an accurate estimate of SDNN,[42,43] therefore, the present analysis focused only on the RS series (5 min).

3.2.3 Poincaré plot (SD1/SD2 ratio)

Poincaré plots were constructed as a delay scatter plot between the intervals RR_i (x-axis) and RR_{i+1} (y-axis), with each point in the plot corresponding to two consecutive RR intervals.[22,44] The Poincaré shapes representing an elongated cloud of points (Fig. 5) around the line-of-identity were evaluated numerically using the ellipse fitting technique. The minor axis of the ellipse perpendicular to line-of-identity is the standard deviation SD1, whereas the major axis is represented by the standard deviation SD2. Analysis was performed using the HRVAS toolbox[41] based on only the RS series (5 min).

3.2.4 Complex correlation measure

The complex correlation method (CCM) was applied to quantify the nonlinear temporal aspects of the Poincaré plot.[23,24] CCM was computed in a windowed manner, which embeds the temporal information of the signal. A moving window of three consecutive points obtained from the Poincaré plot was considered to measure the temporal variation of the points. The detailed mathematical formulation has been previously reported.[23]

4 Results

4.1 Pulse Rate Variability Near-Infrared Spectroscopy and Photoplethysmography

Extraction of PRV_{NIRS} was performed for each of the fNIRS channels 1 to 16 per subject. 13% of the channels over all subjects did not contain cardiac components due to a low signal-to-noise ratio and were excluded from analysis. A single-subject example of the final PRV_{NIRS} estimate obtained by computing the median PRV over all channels at each time point is shown in Fig. 3(a) in comparison to PRV_{PPG}.

Using a general linear model, the beta estimates of the HR in response to the respiratory challenges were calculated per subject and shown on the group-level [Fig. 3(b)]. Results showed that compared to RS, HV (PRV_{NIRS}: $p < 0.001$, PRV_{PPG}: $p < 0.046$) and RB (PRV_{NIRS}: $p < 0.009$, PRV_{PPG}:

(a)

(b)
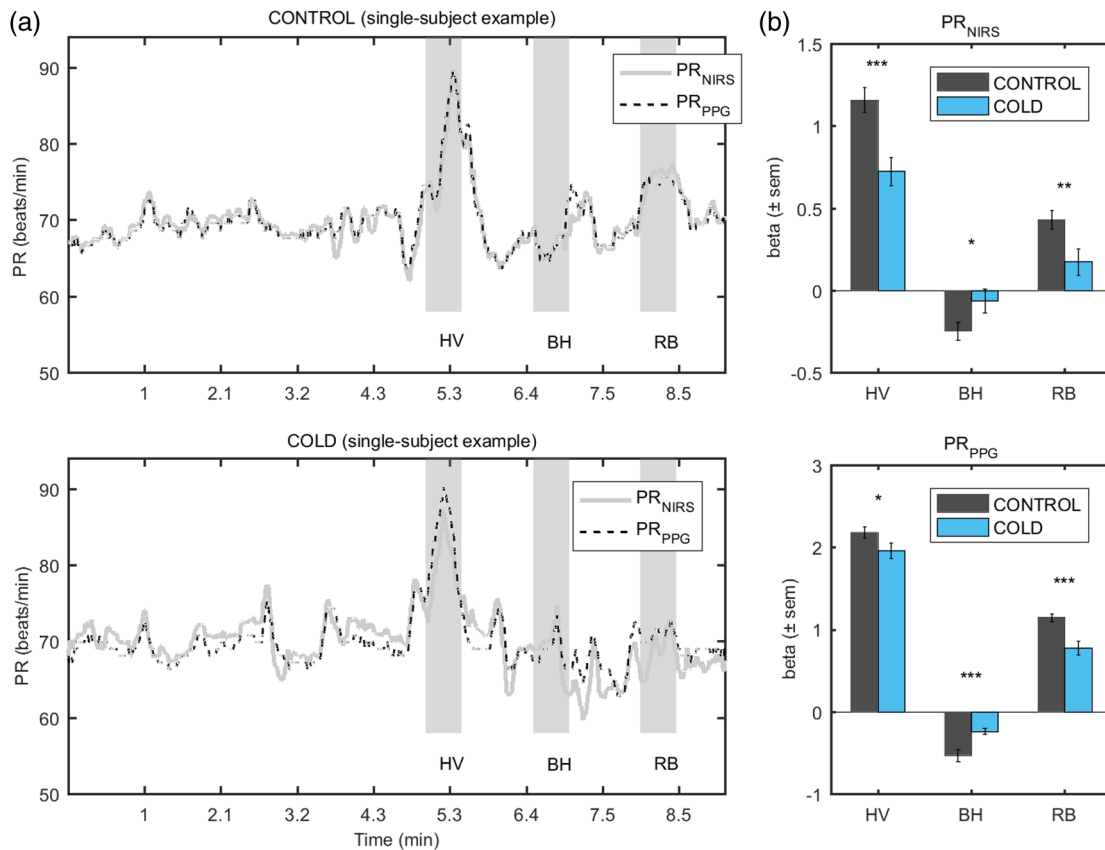
Fig. 3 PR_{NIRS} and PR_{PEG}. (a) Single-subject examples illustrating raw time courses of HR_{NIRS} and HR_{PPG}. (b) Group-level beta estimates of HR responses to respiratory challenges, HV, BH, and RB. Error bars indicate standard error of the mean (SEM). Significance between temperature conditions was highlighted (*).
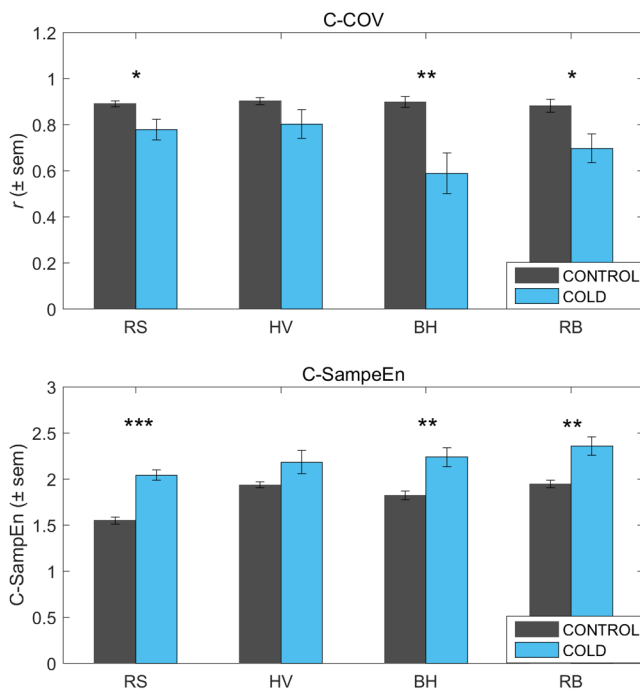
Fig. 4 C-COV and C-SampEn. Group-level results of the accuracy between PRV_{NIRS} and PRV_{PPG} assessed using C-COV and C-SampEn. Error bars indicate SEM. Significant differences between temperature conditions were highlighted (*). See Table 1 for ANOVA.

$p < 0.0001$) induced a larger increase in HR in the CONTROL condition compared to the COLD condition, whereas BH (PRV_{NIRS}: $p = 0.044$, PRV_{PPG}: $p < 0.0001$) induced a smaller HR decrease in condition CONTROL compared to condition COLD. These results indicated that the HR response was overall diminished in the COLD compared to the CONTROL condition.

4.2 Accuracy Between Pulse Rate Variability Measures

The overall correlation between PRV_{NIRS} and PRV_{PPG} was $r > 0.9$. The accuracy between PRV_{NIRS} and PRV_{PPG} was assessed using C-COV and C-SampEn (Fig. 4). Repeated measures ANOVA showed a consistent pattern with significant main effects for both factors "temperature" and "respiration" (Table 1). The between-subject factor "temperature" (CONTROL versus COLD) revealed a smaller main effect for C-COV ($F = 10.026$, $p = 0.005$) compared to C-SampEn ($F = 52.134$, $p < 0.0001$). The within-subject factor "respiration" (RS, HV, BH, and RB) revealed larger C-COV correlation coefficients between PRV_{NIRS} and PRV_{PPG} in the RS in the CONTROL ($r = 0.903$) compared to the COLD ($r = 0.803$) condition. During the respiratory challenges, correlation coefficients decreased with the smallest values in response to BH under both the CONTROL and the COLD condition. Sample entropy represented a mirrored pattern of the correlation analysis, but with an overall larger "temperature" effect, but smaller effects

Table 1 ANOVA C-COV and C-SampEn. Repeated measures ANOVA assessing the accuracy between PRV_{NIRS} and PRV_{PPG} using C-COV and C-SampEn, with the between-subject factor "temperature" (CONTROL versus COLD) and the within-subject factor "respiration" (RS, HV, BH, and RB), followed by *post-hoc* comparisons using paired-test. See Fig. 4 for illustration.

		CONTROL	COLD	CONTROL versus COLD	
		$F = 0.025$	$F = 8.285$		$F = 10.026$
	Main effect "respiration"	$p = 0.877$	$p = 0.018$	Main effect "temperature"	$p = 0.005$
		$\eta_p^2 = 0.003$	$\eta_p^2 = 0.479$		$\eta_p^2 = 0.358$
	RS versus HV	0.674	0.579	RS	0.039
	RS versus BH	0.872	0.024	HV	0.154
	RS versus RB	0.866	0.209	BH	0.005
C-COV	HV versus BH	0.931	0.013	RB	0.033
	HV versus RB	0.721	0.116		
	BH versus RB	0.637	0.327		
		$F = 28.698$	$F = 8.029$		$F = 52.134$
	Main effect "respiration"	$p < 0.001$	$p = 0.020$	Main effect "temperature"	$p < 0.0001$
		$\eta_p^2 = 0.761$	$\eta_p^2 = 0.471$		$\eta_p^2 = 0.743$
	RS versus HV	0.001	0.308	RS	0.000
	RS versus BH	0.025	0.190	HV	0.094
	RS versus RB	0.000	0.030	BH	0.005
C-SampEn	HV versus BH	0.383	0.790	RB	0.004
	HV versus RB	0.927	0.126		
	BH versus RB	0.323	0.511		

of "respiration" indicating less variance between the respiratory challenges.

4.3 Sympathetic and Parasympathetic Autonomous Nervous System Contributions on Pulse Rate Variability

### 4.3.1 Frequency-domain (low frequency/high frequency ratio)

To investigate the frequency aspects that may characterize the contributions of the SNS and PSNS, the HF (0.15 to 0.4 Hz) and LF (0.04 to 0.15 Hz) activities were assessed. Results from the RS indicated that the COLD condition elicited an overall smaller LF/HF ratio compared to the CONTROL condition (Fig. 5). The difference was significant only for PRV_{NIRS} ($p < 0.018$), but not for PRV_{PPG} ($p = 0.829$). The proportional change from the CONTROL to COLD condition was larger in HF activity (76.48%) compared to LF activity (25.48%) (Table 2), indicating that higher HF activity under the COLD condition was the main proportional contributor to the statistical difference. Results obtained from the respiratory challenges showed that the difference in HF activity reached statistical significance only for PRV_{NIRS} for all challenges, but not for PRV_{PPG} (Fig. 6).

4.3.2 Time-domain (SDNN/RMSSD ratio)

Results from the RS in the time-domain indicated that the COLD condition elicited an overall smaller SDNN/RMSSD ratio compared to the CONTROL condition (Fig. 5). The difference was significant only for PRV_{NIRS} ($p = 0.041$), but not for PRV_{PPG} ($p = 0.801$). The proportional change from the CONTROL to COLD condition was larger in RMSSD (27.63%) compared to SDNN (4.24%) (Table 2), indicating that a higher RMSSD index in the COLD condition was the main proportional contributor to the statistical difference. Results obtained from the respiratory challenges showed that the difference in the RMSSD index reached statistical significance only for PRV_{NIRS} for all challenges, but not for PRV_{PPG} (Fig. 6).

4.3.3 Poincaré plot (SD1/SD2 ratio)

Results from the RS of the Poincaré plot revealed that the COLD condition elicited a larger SD1/SD2 ratio compared to the CONTROL condition (Fig. 5). Again, the difference was significant only for PRV_{NIRS} ($p = 0.004$), but not for PRV_{PPG} ($p = 0.690$). The proportional change from the CONTROL to COLD condition was larger in SD1 (18.22%) compared to SD2 (-14.31%) (Table 2), indicating that a higher SD1 index
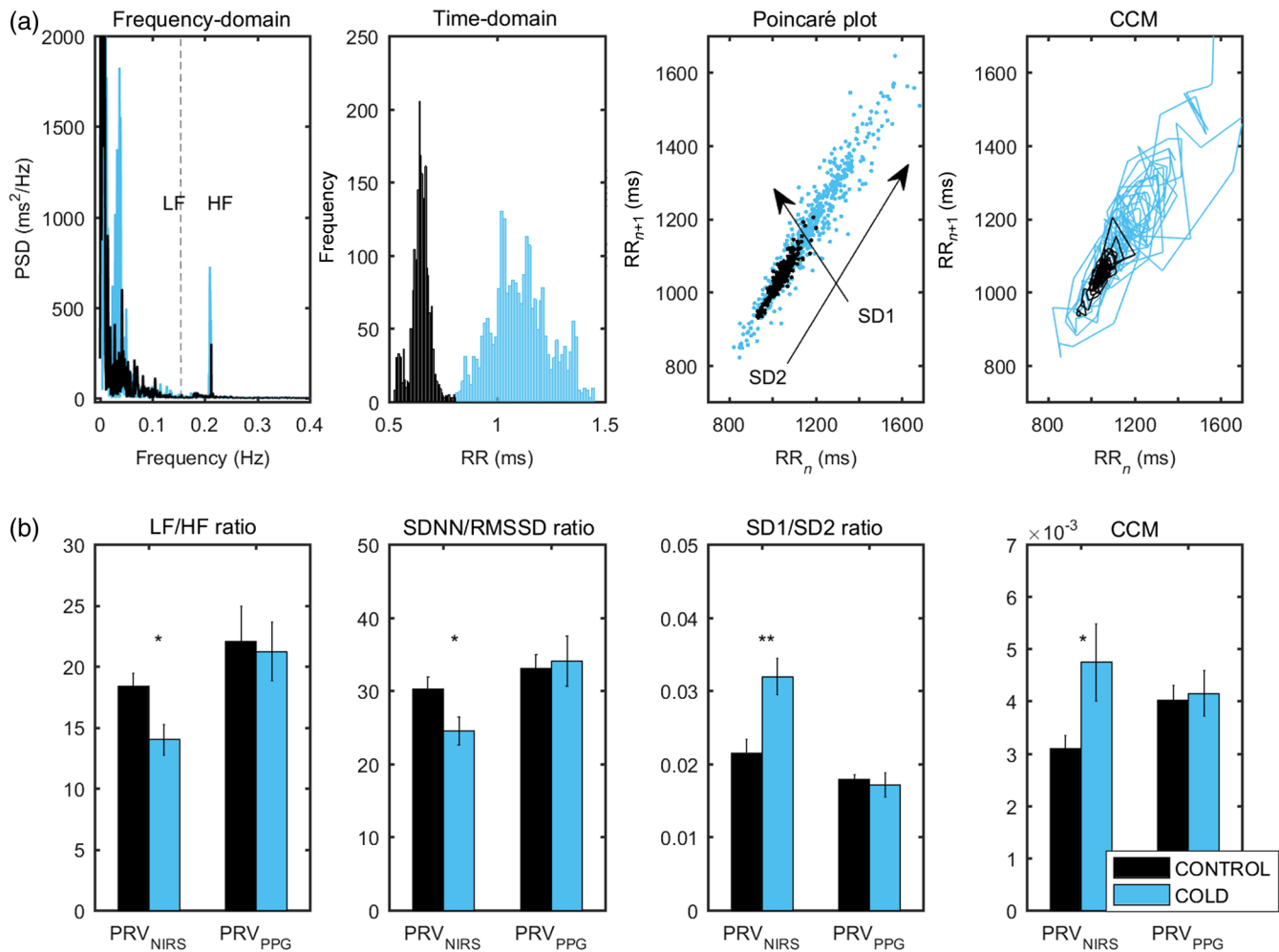
Fig. 5 PRV_{NIRS} and PRV_{PPG} measures (RS). (a) Single-subject level. Examples of the PRV measures assessed in the frequency-domain, the time-domain, the Poincaré plot, and the CCM. (b) Group-level. Bar graphs illustrating the mean $\pm$ SEM of the LF/HF ratio, the SDNN/RMSSD ratio, the SD1/SD2 ratio, and the CCM. Significant differences between temperature conditions were highlighted (*). See Table 2 for statistics.

in the COLD condition was the main proportional contributor to the statistical difference. Results obtained from the respiratory challenges showed that the difference in the SD1 index reached statistical significance only for PRV_{NIRS} for all challenges, but not for PRV_{PPG} (Fig. 6).

4.3.4 Complex correlation measure

The CCM was calculated based on the SD1 and SD2 derived from the Poincaré plot.[23] Results from the RS revealed that the COLD condition elicited a larger CCM value compared to the CONTROL condition (Fig. 5). Again, this difference was significant only for PRV_{NIRS} ($p = 0.047$), but not for PRV_{PPG} ($p = 0.806$).

4.3.5 Receiver operating characteristic for pulse rate variability measures

To illustrate the performance of PRV_{NIRS} and PRV_{PPG} in predicting the temperature change, ROC curves were generated based on logistic regression with the binary classifier "temperature" (CONTROL versus COLD) and the PRV measures as response variables. The AUC values obtained from the RS

showed that PRV_{NIRS} predicted the temperature change better than PRV_{PPG} for all measures, i.e., the LF/HF ratio, the SDNN/RMSSD ratio, the SD1/SD2 ratio, and the CCM (Fig. 7). The differences between AUC reached significance level only for the SD1/SD2 ratio $p < 0.0001$ (LF/HF ratio $p = 0.054$, SDNN/RMSSD ratio $p = 0.069$, and CCM $p = 0.224$). Results obtained from the respiratory challenges confirmed these findings, showing that the AUC values for HF activity, RMSSD, and SD1 were larger for PRV_{NIRS} for most of the challenges compared to PRV_{PPG} (exceptions see Fig. 8).

4.3.6 Correlation between pulse rate variability measures

Pearson correlation coefficients were computed between LF, HF, SDNN, RMSSD, SD1, SD2, and CCM values, for the COLD and CONTROL condition (Fig. 9). Results confirmed that the indices of short-term variability (HF, RMSSD, and SD1) and long-term variability (LF, SDNN, and SD2) exhibited a strong positive correlation each other, and a negative correlation with CCM. The correlations were less stable for PRV_{PPG} under the COLD condition. Results obtained from the respiratory challenges are shown in the Fig. 10.

Table 2 PRV_{NIRS} and PRV_{PPG} measures (RS). Mean/median $\pm$ SEM of LF, HF, SDNN, RMSSD, SD1, SD2, and CCM. Differences between the CONTROL and the COLD condition were assessed using paired t-test. Units are given in milliseconds.

|			CONTROL			COLD			T-test		Proportional change (mean)
			Mean	SEM	Median	Mean	SEM	Median	F	p-value	
Frequency-domain	PRV_{NIRS}	LF	2852.753	588.569	2514.700	3579.560	640.651	3093.000	0.698	0.414	25.48%
		HF	156.343	34.445	130.115	275.921	58.104	217.925	3.134	0.094	76.48%
	PRV_{PPG}	LF	484.164	80.638	390.130	477.207	137.414	328.095	0.002	0.966	−1.44%
		HF	21.344	1.531	21.422	22.738	6.747	12.380	0.041	0.843	6.53%
	PRV_{NIRS}	LF/HF ratio	18.399	1.090	1869.181	14.016	1.275	1348.546	6.826	0.018	
	PRV_{PPG}	LF/HF ratio	22.085	2.903	1851.050	21.254	2.426	2331.723	0.048	0.829	
	PRV_{NIRS}	SDNN	102.090	13.579	82.350	106.420	16.210	106.250	0.042	0.840	4.24%
		RMSSD	3.330	0.339	3.300	4.250	0.508	3.650	2.271	0.149	27.63%
Time-domain	PRV_{PPG}	SDNN	40.080	5.714	37.150	40.540	3.556	37.950	0.005	0.946	1.15%
		RMSSD	1.180	0.106	1.133	1.260	0.138	1.150	0.212	0.651	6.78%
	PRV_{NIRS}	SDNN/RMSSD ratio	30.218	1.772	28.843	24.533	1.884	22.755	4.834	0.041	
	PRV_{PPG}	SDNN/RMSSD ratio	33.117	1.886	31.217	34.106	3.386	32.025	0.065	0.801	
	PRV_{NIRS}	SD1	0.003	0.000	0.003	0.004	0.001	0.003	0.571	0.460	18.22%
		SD2	0.133	0.011	0.119	0.114	0.020	0.079	0.705	0.412	−14.31%
Poincaré plot	PRV_{PPG}	SD1	0.001	0.000	0.001	0.001	0.000	0.001	0.007	0.932	−1.52%
		SD2	0.052	0.006	0.048	0.055	0.004	0.054	0.179	0.678	5.87%
	PRV_{NIRS}	SD1/SD2 ratio	0.022	0.002	0.023	0.032	0.003	0.031	11.204	0.004	
	PRV_{PPG}	SD1/SD2 ratio	0.018	0.001	0.017	0.017	0.002	0.015	0.164	0.690	
CCM	PRV_{NIRS}	CCM	0.003	0.000	0.003	0.005	0.001	0.005	4.492	0.047	
	PRV_{PPG}	CCM	0.004	0.000	0.004	0.004	0.000	0.004	0.062	0.806	
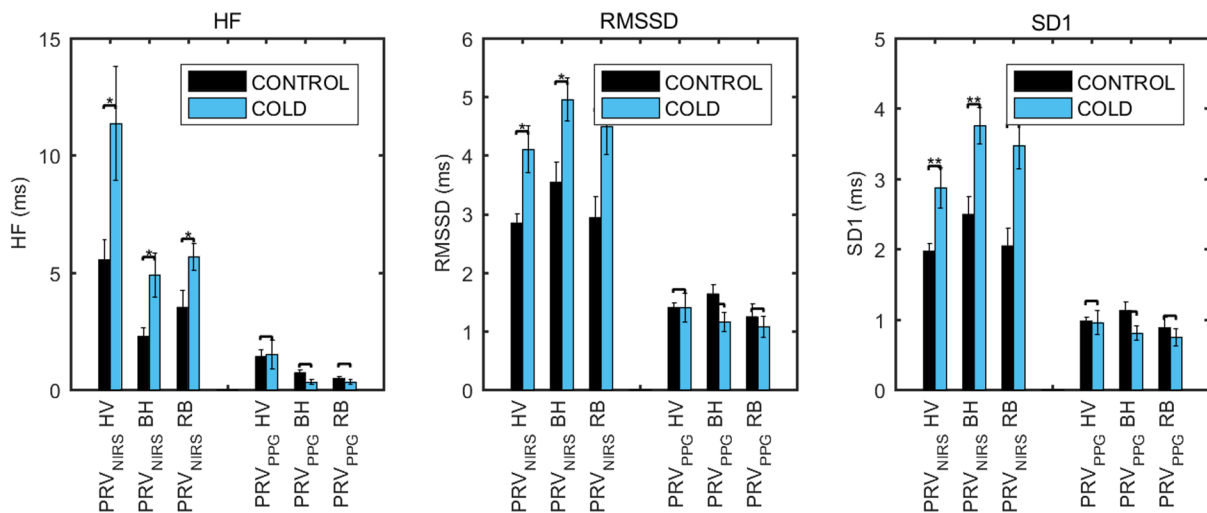
Fig. 6 PRV_{NIRS} and PRV_{PPG} measures (respiratory challenges). Bar graphs illustrating the mean $\pm$ SEM of the short-term variability measures, HF, RMSSD, and SD1, during HV, BH, and RB, for PRV_{NIRS} and PRV_{PPG}. Significant differences between temperature conditions were highlighted (*).
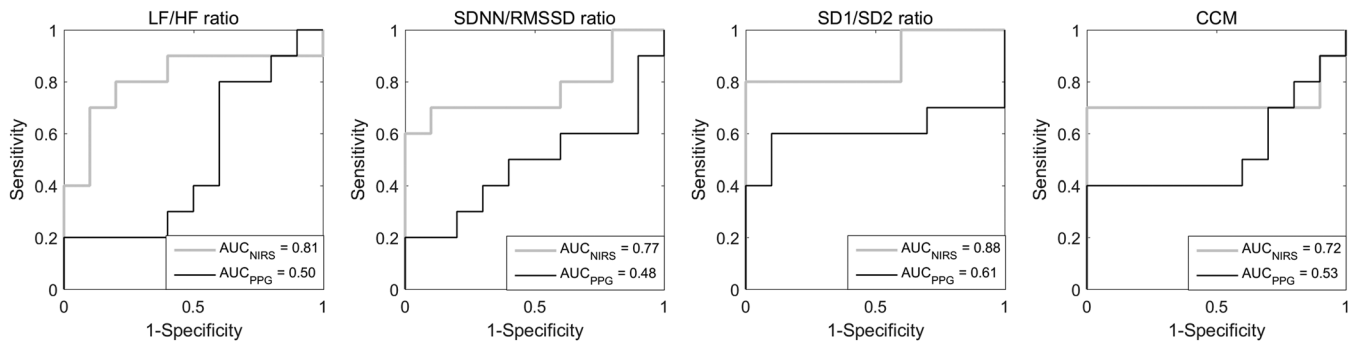
Fig. 7 ROC for PRV_{NIRS} and PRV_{PPG} (RS). Group-level ROC curves and AUC values based on logistic regression with the binary classifier "temperature" (CONTROL versus COLD) for each of the PRV measures, the LF/HF ratio, the SDNN/RMSSD ratio, the SD1/SD2 ratio, and the CCM. Statistical significance of AUC-differences: LF/HF-ratio $p = 0.054$, SDNN/RMSSD ratio $p = 0.069$, SD1/SD2 ratio $p < 0.0001$, CCM $p = 0.224$.

5 Discussion

Previous studies showed that information on the temporal inter-beat-intervals of the heart can be extracted from fNIRS data.[25,26] By comparing simultaneously acquired PRV from NIRS (PRV_{NIRS}) and PRV_{PPG}, the present study showed that PRV_{NIRS} may outperform PRV_{PPG} under conditions involving respiratory and temperature changes. In particular, we show that PRV_{NIRS} may provide a better characterization of the contributions of the SNS and parasympathetic autonomous nervous system compared to PRV_{PPG}, especially regarding the short-term

variability. Extracting PRV_{NIRS} may, therefore, be advantageous for both research and clinical settings as an alternative to PRV_{PPG}.

A main methodological limitation of the present study was that we did not assess simultaneous ECG, the gold standard for investigating PRV. This limitation should be considered when interpreting our results. In 1996, a task force[31] specified standards for calculating PRV measures and reporting results, which have been considered in the present study. Accuracy of the ECG has since then been investigated in numerous studies in health and
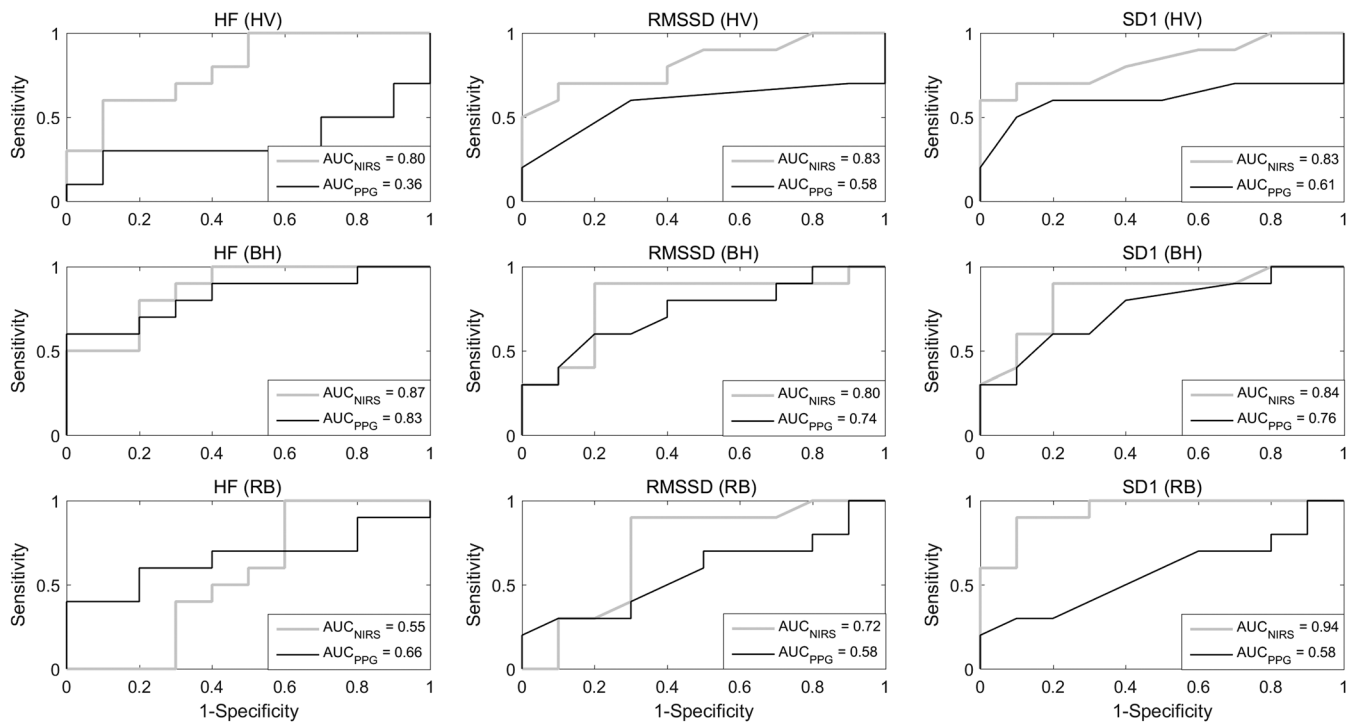
Fig. 8 ROC for PRV_{NIRS} and PRV_{PPG} (respiratory challenges). Group-level ROC curves and AUC values based on logistic regression with the binary classifier "temperature" (CONTROL versus COLD) for each of the short-term variability measures, HF, RMSSD, SD1, during HV, BH, and RB, for PRV_{NIRS} and PRV_{PPG}. Statistical significance of AUC-differences in HV: HF $p = 0.009$, RMSSD $p = 0.015$, SD1 $p = 0.011$; statistical significance of AUC-differences in BH: HF $p < 0.0001$, RMSSD $p < 0.0001$, SD1 $p < 0.0001$; statistical significance of AUC-differences in RB: HF $p = 0.285$, RMSSD $p = 0.091$, SD1 $p < 0.0001$.

CONTROL PRV_{NIRS} (r)

	LF	HF	SDNN	RMSSD	SD1	SD2	CCM
LF	1.00	0.93	0.51	0.53	0.39	0.16	-0.09
HF	0.93	1.00	0.43	0.41	0.31	0.09	-0.21
SDNN	0.51	0.43	1.00	0.89	0.90	0.87	-0.60
RMSSD	0.53	0.41	0.89	1.00	0.97	0.80	-0.49
SD1	0.39	0.31	0.90	0.97	1.00	0.88	-0.57
SD2	0.16	0.09	0.87	0.80	0.88	1.00	-0.74
CCM	-0.09	-0.21	-0.60	-0.49	-0.57	-0.74	1.00

CONTROL PRV_{PPG} (r)

	LF	HF	SDNN	RMSSD	SD1	SD2	CCM
LF	1.00	0.65	0.88	0.94	0.91	0.88	-0.51
HF	0.65	1.00	0.66	0.81	0.75	0.63	-0.17
SDNN	0.88	0.66	1.00	0.93	0.98	0.99	-0.80
RMSSD	0.94	0.81	0.93	1.00	0.97	0.92	-0.53
SD1	0.91	0.75	0.98	0.97	1.00	0.95	-0.67
SD2	0.88	0.63	0.99	0.92	0.95	1.00	-0.81
CCM	-0.51	-0.17	-0.80	-0.53	-0.67	-0.81	1.00

COLD PRV_{NIRS} (r)

	LF	HF	SDNN	RMSSD	SD1	SD2	CCM
LF	1.00	0.94	0.58	0.57	0.58	0.41	-0.18
HF	0.94	1.00	0.47	0.46	0.49	0.33	-0.18
SDNN	0.58	0.47	1.00	0.87	0.96	0.94	-0.48
RMSSD	0.57	0.46	0.87	1.00	0.87	0.73	-0.09
SD1	0.58	0.49	0.96	0.87	1.00	0.92	-0.40
SD2	0.41	0.33	0.94	0.73	0.92	1.00	-0.70
CCM	-0.18	-0.18	-0.48	-0.09	-0.40	-0.70	1.00

COLD PRV_{PPG} (r)

	LF	HF	SDNN	RMSSD	SD1	SD2	CCM
LF	1.00	0.91	0.38	0.97	0.91	0.16	0.75
HF	0.91	1.00	0.28	0.85	0.75	0.14	0.69
SDNN	0.38	0.28	1.00	0.48	0.64	0.95	-0.25
RMSSD	0.97	0.85	0.48	1.00	0.97	0.26	0.71
SD1	0.91	0.75	0.64	0.97	1.00	0.42	0.57
SD2	0.16	0.14	0.95	0.26	0.42	1.00	-0.46
CCM	0.75	0.69	-0.25	0.71	0.57	-0.46	1.00

Fig. 9 Correlation between PRV measures (RS). Pearson correlation coefficients for PRV_{NIRS} and PRV_{PPG} between LF, HF, SDNN, RMSSD, SD1, SD2, and CCM values, for the CONTROL and the COLD conditions.

CONTROL PRV_{NIRS}

HV
	HF	RMSSD	SD1
HF	1.00	0.57	0.45
RMSSD	0.57	1.00	0.97
SD1	0.45	0.97	1.00

BH
	HF	RMSSD	SD1
HF	1.00	0.57	0.54
RMSSD	0.57	1.00	1.00
SD1	0.54	1.00	1.00

RB
	HF	RMSSD	SD1
HF	1.00	0.85	0.84
RMSSD	0.85	1.00	1.00
SD1	0.84	1.00	1.00

CONTROL PRV_{PPG}

HV
	HF	RMSSD	SD1
HF	1.00	0.72	0.64
RMSSD	0.72	1.00	0.95
SD1	0.64	0.95	1.00

BH
	HF	RMSSD	SD1
HF	1.00	0.35	0.35
RMSSD	0.35	1.00	1.00
SD1	0.35	1.00	1.00

RB
	HF	RMSSD	SD1
HF	1.00	0.72	0.72
RMSSD	0.72	1.00	1.00
SD1	0.72	1.00	1.00

COLD PRV_{NIRS}

HV
	HF	RMSSD	SD1
HF	1.00	0.50	0.46
RMSSD	0.50	1.00	1.00
SD1	0.46	1.00	1.00

BH
	HF	RMSSD	SD1
HF	1.00	0.05	0.05
RMSSD	0.05	1.00	1.00
SD1	0.05	1.00	1.00

RB
	HF	RMSSD	SD1
HF	1.00	0.61	0.60
RMSSD	0.61	1.00	1.00
SD1	0.60	1.00	1.00

COLD PRV_{PPG}

HV
	HF	RMSSD	SD1
HF	1.00	0.95	0.93
RMSSD	0.95	1.00	0.99
SD1	0.93	0.99	1.00

BH
	HF	RMSSD	SD1
HF	1.00	0.73	0.67
RMSSD	0.73	1.00	0.99
SD1	0.67	0.99	1.00

RB
	HF	RMSSD	SD1
HF	1.00	0.93	0.93
RMSSD	0.93	1.00	1.00
SD1	0.93	1.00	1.00

Fig. 10 Correlation between PRV measures (respiratory challenges). Pearson correlation coefficients for PRV_{NIRS} and PRV_{PPG} between the short-term variability measures, HF, RMSSD, and SD1, for the CONTROL and the COLD conditions.

disease,[1-4] and the correlation with both PRV_{PPG}[7] and PRV_{NIRS}[25] under resting conditions has been reported to be high.

5.1 Accuracy Between Pulse Rate Variability Measures

To compare the accuracy between PRV_{NIRS} and PRV_{PPG}, the present analysis assessed C-COV and C-SampEn. C-COV showed the relative correlations between the PRV_{NIRS} and PRV_{PPG}, whereas C-SampEn reflected the regularity between the two PRV measures. Overall, we found good agreement between the two methods with the largest coefficients under RS ($r = 0.903$). However, both changes in respiration and temperature resulted in reduced correlation (C-COV) and stronger irregularity (C-SampEn) between PRV_{NIRS} and PRV_{PPG} (Fig. 4 and Table 1). The lower correlation in response to respiratory and temperature changes may reflect the previously reported inaccuracy of PRV_{PPG} under nonoptimal conditions, such as including motion artifacts,[6] physical strenuous exercise,[5] or mental stressors.[7] Although our subjects were instructed to keep the body as still as possible during the respiratory challenges, the breathing and temperature changes certainly induced minor body motions and mental stress, respectively, that may have contributed to the inaccuracy of PRV_{PPG}. The PRV_{NIRS} signal shows more high-frequency variability compared to PRV_{PPG}. That this high-frequency variability contains some physiological relevant information (i.e., diminished in the PRV_{PPG} data) is a shown by the present results.

It should further be mentioned that the correlations between PRV_{NIRS} and PRV_{PPG} were slightly lower than that has been reported previously in adult[25] and infant data.[26] These differences may arise due the difference between PPG (applied in our study) versus EEG (applied in the two other studies).

5.2 Sympathetic and Parasympathetic Autonomous Nervous System Contributions on Pulse Rate Variability

To characterize the contributions of the SNS or PSNS on PRV_{NIRS} and PRV_{PPG} in response to the temperature change, we applied frequency- and time-domain measures based on linear and nonlinear methods.

In general, exposure to cold temperature changes the relationship between the SNS or PSNS. Whereas the PSNS (the "rest and digest" system) restores the body's energy primarily associated with decreases in PRV, the SNS (the "fight and flight" system) is primarily associated with increases in PRV. Furthermore, although the effect on PRV of cooling varies with the duration of the temperature change, it is thought that cold exposure modulates short-term variability (i.e., HF, RMSSD, and SD1) more than long-term variability (LF, SDNN, and SD2).[8] This indicates that cold exposure modulates SNS-PSNS balance by causing a shift toward increased PSNS activity. Previous studies comparing PRV derived from PPG and ECG under optimal rest conditions did not report significant differences in PRV assessment.[6,45,46] However, studies that compared PPG and ECG under less optimal conditions have shown that PRV_{PPG} assessed the parameters of short-term variability (HF, RMSSD, and SD1) considerable less reliable compared to ECG.[7,9]

In line with these findings, our results showed that the cold temperature change (COLD) exhibited significant increases of the parameters reflecting short-term variability (i.e., HF activity, RMSSD, and SD1), whereas the parameters reflecting long-term variability did not change significantly compared to the control condition (CONTROL). Importantly, these differences between the cold and control temperature could only be significantly characterized by PRV_{NIRS}, but not by PRV_{PPG}. Furthermore, the better performance in characterizing short-term variability of PRV_{NIRS} compared to PRV_{PPG} was not only observed under potentially stressful respiratory challenges (Figs. 6 and 8), but were even detectable under RS conditions (Fig. 5 and Table 2). The ROC analysis confirmed these results indicating that PRV_{NIRS} had a better predictive power to differentiate the temperature change compared to PRV_{PPG}, with the SD1/SD2 ratio obtained from the Poincaré plot revealing the best discrimination (AUC-/ROC-differences, Fig. 7).

Together, our results indicated that PRV_{NIRS} had a significantly higher sensitivity to the short-term contributions of the PSNS compared to PRV_{PPG}. These findings show that under conditions which may induce changes primarily in short-term variability, both research and clinical settings may benefit from using PRV_{NIRS} to overcome the lower reliability of PRV_{PPG}. That the PRV_{NIRS} signal contains more high-frequency information than PRV_{PPG} can also be easily see in Fig. 3.

5.3 Methodological Considerations and Limitations

Core and skin temperature are the body's two temperature components. Core temperature (T_c) represents the internal or deep body temperature, whereas skin temperature represents the mean outside surface body temperature (T_{sk}). The average temperature of the body at any time is a weighted balance between these two temperature components. When confronted with thermal stress (heat or cold), the body strives to control T_c through physiological adjustments, and T_{sk} provides the major feedback to the brain to coordinate this control.

While T_{sk} varies greatly with ambient temperature, T_b is relatively stable. When T_{sk} decreases, HR in general goes down due to a parasympathetic reflex.[47] However, if the cold stress is of sufficient magnitude to decrease T_c, HR may either increase (due to sympathetic activation) or decrease (due to increased central blood volume). Regarding the present study, we hypothesized that the cold temperature change was not strong enough to affect T_c (although, this hypothesis could not be confirmed, since we did not directly assess T_{sk} or T_c). Therefore, the induced cold temperature change in this study was hypothesized to decrease T_{sk} only. In line with this assumption, we found that HR amplitudes were significantly reduced in response to the cold temperature change (Fig. 3), most likely reflecting a general HR slowdown due to the assumed increase in PSNS activity.[8,47]

5.4 Conclusion

By comparing simultaneously acquired PRV_{NIRS} and PRV_{PPG}, the present study showed that PRV_{NIRS} may outperform PRV_{PPG} under conditions involving respiratory and temperature changes. In particular, our results indicated that PRV_{NIRS} may provide a better characterization of the short-term contributions of the autonomous nervous system compared to PRV_{PPG}. Extracting PRV_{NIRS} may, therefore, be advantageous for both research and clinical settings, while being a brain imaging method at the same time.

References

1. H. V. Huikuri and P. K. Stein, "Heart rate variability in risk stratification of cardiac patients," *Ambul. ECG Monit. Clin. Pract. Res. Appl.* **56**, 153–159 (2013).
2. G. Prinsloo, H. Rauch, and W. Derman, "A brief review and clinical application of heart rate variability biofeedback in sports, exercise, and rehabilitation medicine," *Phys. Sportmed.* **42**, 88–99 (2014).
3. J. Sacha, "Interaction between heart rate and heart rate variability," *Ann. Noninvasive Electrocardiol.* **19**, 207–216 (2014).
4. C. da Silva et al., "The effect of physical training on heart rate variability in healthy children: a systematic review with meta-analysis," *Pediatr. Exercise Sci.* **26**, 147–158 (2014).
5. Y. Iyriboz et al., "Accuracy of pulse oximeters in estimating heart rate at rest and during exercise," *Br. J. Sports Med.* **25**, 162–164 (1991).
6. G. Lu and F. Yang, "Limitations of oximetry to measure heart rate variability measures," *Cardiovasc. Eng.* **9**, 119–125 (2009).
7. A. Schäfer and J. Vagedes, "How accurate is pulse rate variability as an estimate of heart rate variability? a review on studies comparing photoplethysmographic technology with an electrocardiogram," *Int. J. Cardiol.* **166**, 15–29 (2013).
8. T. Mäkinen et al., "Autonomic nervous function during whole-body cold exposure before and after cold acclimation," *Aviat. Space Environ. Med.* **79**, 875–882 (2008).
9. W.-H. Lin et al., "Comparsion of heart rate variability from PPG with that from ECG," *The International Conference on Health Informatics*, Y.-T. Zhang, ed., Vol. **42**, pp. 213–215, Springer International Publishing, New York (2014).
10. P. Grossman and S. Svebak, "Respiratory sinus arrhythmia as an index of parasympathetic cardiac control during active coping," *Psychophysiology* **24**, 228–235 (1987).
11. P. Grossman, J. Karemaker, and W. Wieling, "Prediction of tonic parasympathetic cardiac control using respiratory sinus arrhythmia: the need for respiratory control," *Psychophysiology* **28**, 201–216 (1991).
12. P. G. Katona and F. Jih, "Respiratory sinus arrhythmia: noninvasive measure of parasympathetic cardiac control," *J. Appl. Physiol.* **39**, 801–805 (1975).
13. A. E. Hedmann et al., "The high frequency component of heart rate variability reflects cardiac parasympathetic modulation rather than parasympathetic 'tone'," *Acta Physiol. Scand.* **155**, 267–273 (1995).
14. G. E. Billman, "The LF/HF ratio does not accurately measure cardiac sympatho-vagal balance," *Front. Physiol.* **4**, 26 (2013).
15. A. Malliani et al., "Cardiovascular neural regulation explored in the frequency domain," *Circulation* **84**, 482–492 (1991).
16. M. Pagani et al., "Power spectral density of heart rate variability as an index of sympatho-vagal interaction in normal and hypertensive subjects," *J. Hypertens.* **2**, S383–S385 (1984).
17. M. Pagani et al., "Power spectral analysis of heart rate and arterial pressure variabilities as a marker of sympatho-vagal interaction in man and conscious dog," *Circ. Res.* **59**, 178–193 (1986).
18. M. Doret et al., "Fractal analysis and hurst parameter for intrapartum fetal heart rate variability analysis: a versatile alternative to frequency bands and LF/HF ratio," *PLoS ONE* **10**, e0136661 (2015).
19. D. Saboul, V. Pialoux, and C. Hautier, "The breathing effect of the LF/HF ratio in the heart rate variability measurements of athletes," *Eur. J. Sport Sci.* **14**, S282–S288 (2014).
20. H. Wang and S. Huang, "SDNN/RMSSD as a surrogate for LF/HF: a revised investigation," *Model. Simul. Eng.* **2012**, 931943 (2012).
21. R. Balocchi et al., "Revisiting the potential of time-domain indexes in short-term HRV analysis," *Biomed. Tech.* **51**, 190–193 (2006).
22. M. Brennan, M. Palaniswami, and P. Kamen, "Do existing measures of Poincare plot geometry reflect nonlinear features of heart rate variability?," *IEEE Trans. Biomed. Eng.* **48**, 1342–1347 (2001).
23. C. K. Karmakar et al., "Complex correlation measure: a novel descriptor for Poincaré plot," *Biomed. Eng. OnLine* **8**, 17 (2009).
24. C. K. Karmakar et al., "Sensitivity of temporal heart rate variability in Poincaré plot to changes in parasympathetic nervous system activity," *Biomed. Eng. OnLine* **10**, 17 (2011).
25. I. Trajkovic, F. Scholkmann, and M. Wolf, "Estimating and validating the interbeat intervals of the heart using near-infrared spectroscopy on the human forehead," *J. Biomed. Opt.* **16**, 087002 (2011).
26. K. L. Perdue et al., "Extraction of heart rate from functional near-infrared spectroscopy in infants," *J. Biomed. Opt.* **19**, 067010 (2014).
27. H. ChuDuc, K. NguyenPhan, and D. NguyenViet, "A review of heart rate variability and its applications," in *3rd Int. Conf. Biomedical Engineering Technology (ICBET 2013)*, Vol. 7, pp. 80–85 (2013).
28. A. Singh et al., "Spatial registration of multichannel multi-subject fNIRS data to MNI space without MRI," *NeuroImage* **27**, 842–851 (2005).
29. M. Xia, J. Wang, and Y. He, "BrainNet viewer: a network visualization tool for human brain connectomics," *PLoS ONE* **8**, e68910 (2013).
30. F. Scholkmann, J. Boss, and M. Wolf, "An efficient algorithm for automatic peak detection in noisy periodic and quasi-periodic signals," *Algorithms* **5**, 588–603 (2012).
31. Task force of the European Society of Cardiology the North American Society of Pacing Electrophysiology, "Heart rate variability: standards of measurement, physiological interpretation, and clinical use," *Circulation* **93**, 1043–1065 (1996).
32. D. Singh et al., "Effects of RR segment duration on HRV spectrum estimation," *Physiol. Meas.* **25**, 721–735 (2004).
33. C. C. Grant et al., "Importance of tachogram length and period of recording during noninvasive investigation of the autonomic nervous system," *Ann. Noninvasive Electrocardiol.* **16**, 131–139 (2011).
34. S. M. Pincus, "Approximate entropy as a measure of system complexity," *Proc. Natl. Acad. Sci.* **88**, 2297–2301 (1991).
35. P. Li et al., "Testing pattern synchronization in coupled systems through different entropy-based measures," *Med. Biol. Eng. Comput.* **51**, 581–591 (2013).
36. T. Zhang, Z. Yang, and J. Coote, "Cross-sample entropy statistic as a measure of complexity and regularity of renal sympathetic nerve activity in the rat," *Exp. Physiol.* **92**, 659–669 (2007).
37. M. Aktaruzzaman and R. Sassi, "Parametric estimation of sample entropy in heart rate variability analysis," *Biomed. Signal Process. Control* **14**, 141–147 (2014).
38. D. E. Lake et al., "Sample entropy analysis of neonatal heart rate variability," *Am. J. Physiol. Regul. Integr. Comp. Physiol.* **283**, R789–R797 (2002).
39. M. Weippert et al., "Sample entropy and traditional measures of heart rate dynamics reveal different modes of cardiovascular control during low intensity exercise," *Entropy* **16**, 5698–5711 (2014).
40. Y. İşler and M. Kuntalp, "Combining classical HRV indices with wavelet entropy measures improves to performance in diagnosing congestive heart failure," *Comput. Biol. Med.* **37**, 1502–1510 (2007).
41. J. Ramshur, *Design, Evaluation, and Application of Heart Rate Variability Analysis Software (HRVAS)*, University of Memphis, Memphis, Tennessee (2010).
42. M. R. Esco and A. A. Flatt, "Ultra-short-term heart rate variability indexes at rest and post-exercise in athletes: evaluating the agreement with accepted recommendations," *J. Sports Sci. Med.* **13**, 535–541 (2014).
43. T. Thong et al., "Accuracy of ultra-short heart rate variability measures," in *Engineering in Medicine and Biology Society, 2003. Proc. of the 25th Annual Int. Conf. of the IEEE*, Vol. 3, pp. 2424–2427 (2003).
44. C. K. Karmakar et al., "Analyzing temporal variability of standard descriptors of Poincaré plots," *J. Electrocardiol.* **43**, 719–724 (2010).
45. M. Bolanos, H. Nazeran, and E. Haltiwanger, "Comparison of heart rate variability signal features derived from electrocardiography and photoplethysmography in healthy individuals," in *Engineering in Medicine and Biology Society, 2006. EMBS '06. 28th Annual Int. Conf. of the IEEE*, pp. 4289–4294 (2006).
46. N. Selvaraj et al., "Assessment of heart rate variability derived from finger-tip photoplethysmography as compared to electrocardiography," *J. Med. Eng. Technol.* **32**, 479–484 (2008).
47. J. LeBlanc, *Man in the Cold*, Charles C Thomas Publishing, Springfield, IL (1975).

Lisa Holper is a resident physician at the Department of Psychiatry, Psychotherapy, and Psychosomatics, Hospital of Psychiatry Zurich,

University Zurich. She has published and contributed to over 30 papers addressing human research in healthy and psychiatric populations, particularly in the field of optical brain imaging.

Erich Seifritz is the director of the Department of Psychiatry, Psychotherapy, and Psychosomatics, Hospital of Psychiatry Zurich, University Zurich. He has published and contributed to over 100 papers addressing animal and human research on psychiatric populations in the fields of neuroimaging, brain stimulation, genetics, and neuroeconomics.

Felix Scholkmann is a postdoctoral researcher at the Biomedical Optics Research Laboratory, University Hospital Zurich, University of Zurich. He has published and contributed to over 30 papers addressing the technical development and application of fNIRS-based optical brain imaging and physiological monitoring.